

## THE EFFECT OF THE TYPES OF SUPPORTS IN THE DISTRIBUTION OF LOADS BETWEEN THE GIRDERS OF THE BRIDGE

Mohammed Hassan, Khalil AL-Bukhaiti\* and Deshan Shan

School of Civil Engineering, south west Jiaotong University, Chengdu, Sichuan, China.

---

**ABSTRACT:** *The paper includes three-dimensional nonlinear analysis for reinforced concrete bridge deck consisting of three main girders. The finite brick element is used to predict the response of the bridge under monotonically increasing static loads up to failure. The primary interest is given to the effects of boundary conditions at the supports, and their effects on the behavior of the bridge. Three types of supports were considered, these are simple support, elastomeric pads, and a simple springs. The study also includes the effect of boundary conditions on the failure load, the load distribution amongst the main girders, and variation of bearing reactions in both pre and post-cracking phases. The study presented that the method of representing the supports significantly affects the distribution of the loads among the main girders of the bridge.*

**KEYWORDS:** Bearings, Bridge, Finite Element, Load Distribution, Nonlinear Analysis, Reinforced Concrete.

---

### INTRODUCTION

Finite element method always considered as a powerful and versatile tool for the analysis of complex structures like bridges and it is capable of taken cognizance of material nonlinearly, cracking and the three-dimensional nature of the problem.

Bakht and Jaeger [1] used a plane-shell finite element to analyze I-section of the steel girder bridge by using numerous values of bearing restraints. However, it has been noticed that the main reason that existing bridges on the ground proved to be stiffer than their actual calculated design values is simply because of the presence of horizontal restraint offered by girder supports. Tarhini and Frederick [2] used the finite element method to predict the actual stress distribution and evaluate the load transfer to the beams of a highway bridge from designed vehicle loads.

Mahmood [3] used nine-node shell elements to investigate the exacted behavior of reinforced concrete girder bridges under monotonically increasing load up to failure. The study also includes prediction of the distribution of the load amongst the main girders during different stages of loading, a variation of the support reactions in the pre and post-cracking stages and the effect of the number of cross beams and their locations on the overall response of the bridge.

Kwasniewski [4] Show finite solid element analysis of a deck girder bridge. It got that the boundary condition at the girder's ends is the, more importantly, a given parameter in the modeling of the bridge system under service load. Partial constraints at the supports were simulated by the use of spring elements.

In current study, many approaches have been made to investigate the critical impact of

simulation of bridge supports on the overall response of reinforced concrete deck girder bridges under increasing load up to failure. Nonlinear analysis can be conducted using 20 node brick finite elements to represent the concrete while reinforcement bars are represented by smeared layers. Three types of modeling were used to represent the simple supports.

### MATERIALS MODELING

Concrete in compression considered to behave as linear elastic up to about  $0.3f'_c$  followed by a plastic response with strain hardening model [5] as shown in Fig. (1). The action of concrete in tension is considered as elastic linear up to cracking stress. An exponential stress degradation function is used to model the tension stiffening that allows the post-cracking tensile stress in concrete to be retained in the cracked concrete [6]. Also, shear retention under further loading in post-cracking stages is used to model the shear transfer through cracks.

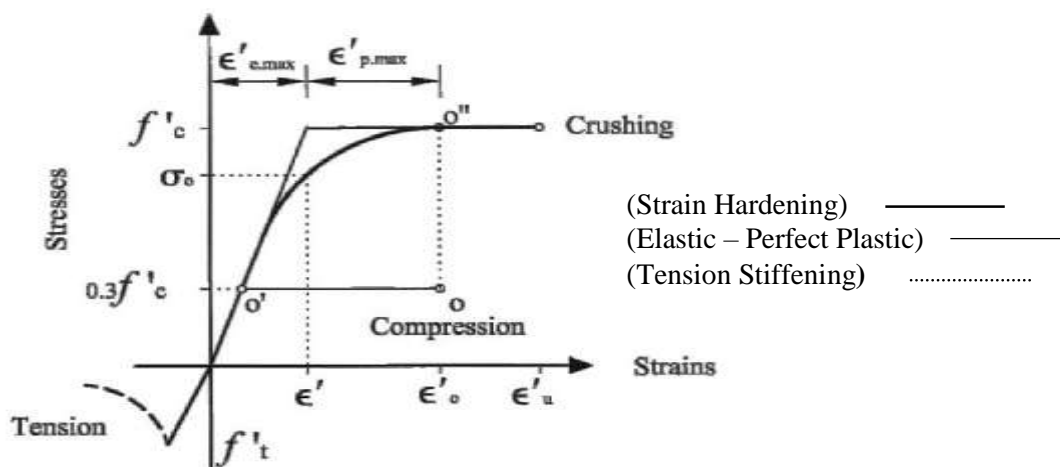


**Fig. (1) Uniaxial representation of the concrete constitutive model**

Steel material has been treated as elastic-perfectly plastic or as an elastic linear strain hardening material [7].

Rubber, when confined, it is almost incompressible, and for practical purposes, its volume does not alter under load, therefore for such material to deform under particular loading it must be able to bulge laterally [8] as shown in Fig. (2).

Poisson's ratio  $\nu$  for elastomeric is taken equal to 0.49 [9], and in the present study the following properties have been used to model the material properties of the elastomer [10,11]:

Hardness IRHD2	Young's Modulus MPa	Shear Modulus (G) MPa	Material Compressibility Coefficient $\emptyset$	Bulk Modulus ( $E_b$ ) MPa
60	4.45	1.06	0.57	1150

### Finite Element Models

20-node isoperimetric brick elements were used to represent the concrete.

The contribution to the stiffness matrix from the solid concrete element is determined by the expression [12]:

$$[K_c] = \iiint_{-1}^{+1} [B]^T \cdot [D_c] \cdot [B] \cdot |J| d\xi d\eta d\zeta \quad (1)$$

The reinforcement is represented by a smeared layer having a thickness equivalent to the area of steel bars, as shown in Fig. (3).

The stiffness contribution of each layer is evaluated by using (2\*2) Gauss quadrature rule:

$$[K_s] = \iint_{-1}^{+1} [B]^T \cdot [D_s] \cdot [B] th |J_s| d\xi d\eta \quad (2)$$

Its stiffness is added to that of the concrete to obtain the total stiffness of the element so that:

$$[K_T] = [K_c] + [K_s] \quad (3)$$

Representation of elastomeric Pad bearings:

The elastomeric pad bearing for girder bridges consists of one or more internal layers of elastomer bonded to internal steel laminates of rectangular shape by the process of vulcanization. The components of a typical elastomeric pad bearing are shown in Fig. (4) [8].

In the present study the adopted dimensions of elastomeric pad bearing are:

Plan dimensions (a\*b) = 300\*300 mm

Total thickness (h) = 52 mm

The thickness of individual elastomer layer (h<sub>i</sub>) = 10 mm

No. of internal elastomer layers = 3

No. of laminates = 4

The thickness of each laminate (h<sub>s</sub>) = 3 mm

The thickness of top or bottom cover (h<sub>c</sub>) = 5 mm

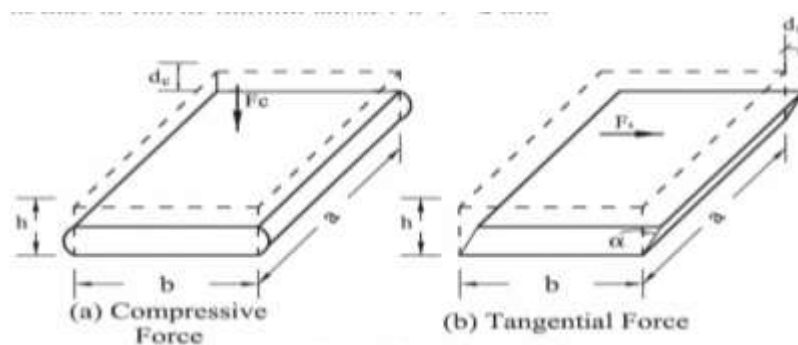


**Fig. (2) Basic deformations of elastomeric bearings under load.**

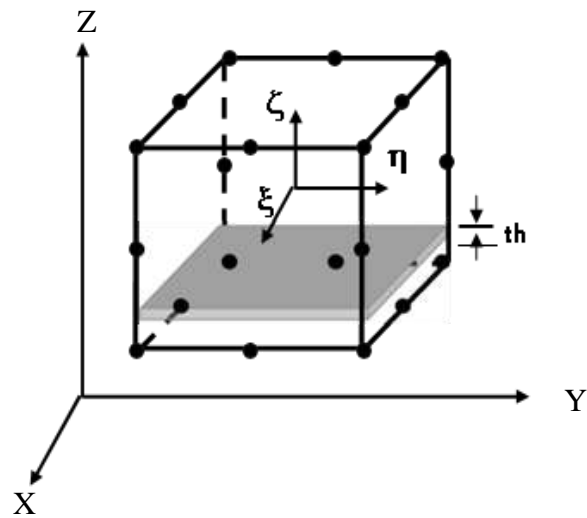


**Fig. (3) A twenty-noded isoperimetric solid element with reinforcement**

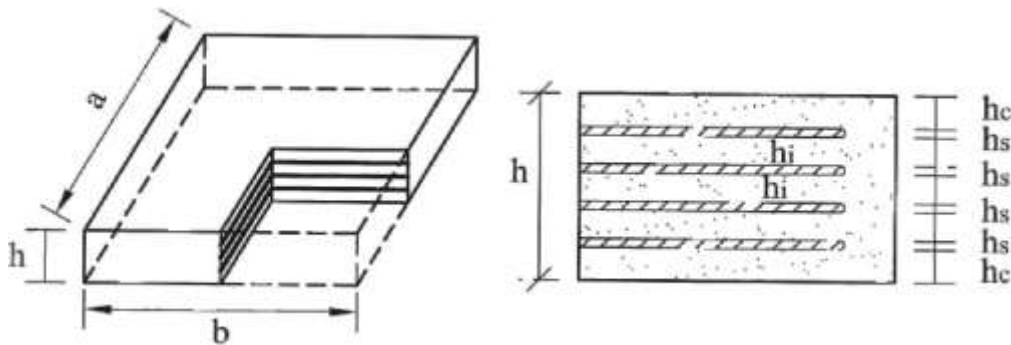


**Fig. (4) Components of elastomeric pad bearing**

Two approaches are used to describe the elastomeric bearing; these are briefly explained below [13]:

- 1- Each pad is represented by 3-D finite brick elements with twenty nodes and steel laminates represented by smeared layers. Each layer is located at its exact location at a constant distance from the neutral axis of the element.

The stiffness of these elements, which represent the bearings, is added to the global stiffness of the structure. Perfect bond is assumed between the top nodes of the elastomeric bearing element with the bottom nodes of girder element by assigning the same nodes numbering, while the bottom nodes of the elements representing elastomeric bearing assumed to be fixed.

Deformations, strains, and stresses for these bearing elements are calculated at different stages of loading.

- 2- In the second approach vertical and horizontal springs, with proper stiffness are used to represent the elastomeric supports. The stiffness of these springs are calculated as given below [11]:

$$K_s = \frac{F_s}{d_s} = \frac{A \cdot G}{h} \quad (4)$$

$$K_v = \frac{F_c}{d_c} = \frac{A \cdot E_r}{h} \quad (5)$$

Where:

- A is the loaded area.
- G is the shear modulus of rubber.
- h is the total thickness of the elastomeric support.
- Er is the effective compression modulus, and the relation gives it:

$$E_r = E_o(1 + 2\phi S^2) \quad (6)$$

Where:

- $E_o$  is the Young's modulus of rubber.
- $\phi$  is the material compressibility coefficient of rubber.
- S is the shape factor which is given as:

$$S = \frac{\text{Load Area}}{\text{bulge Area}} = \frac{(\text{Length}) \times (\text{Width})}{2 \cdot h_i \cdot (\text{Length} + \text{Width})} \quad (7)$$

The following factor should multiply the calculated compression modulus:  $\frac{1}{1+E_o/E_b}$

Where:

- $E_b$  is the bulk modulus of rubber.

Results from this method of calculating compression modulus are summarized graphically in Fig. (5) [11]. This graph can be used to find out the effective compression modulus for the components.

After calculating the values of the vertical and horizontal stiffness of these specific springs, the elastomeric supports replaced by these springs are as depicted in Fig. (6).

Normally, these particular springs are connected to the bottom nodes of the first element of each girder located at the two ends of the bridge. This procedure can only be achieved ideally by producing the first element size equal to the dimension of the elastomeric support.

In the current study, the numerical integration for evaluating the element matrices is carried out using the 15-Gauss points rule distributed over the volume of the brick element [14].

The nonlinear equations of equilibrium are analytically computed by using an incremental-iterative technique based on the modified Newton-Raphson approach in which the tangent

stiffness matrix is computed in the first iteration for each load increment. The convergence of the nonlinear solution is controlled by a displacement convergence criterion, where 2% tolerance is considered.

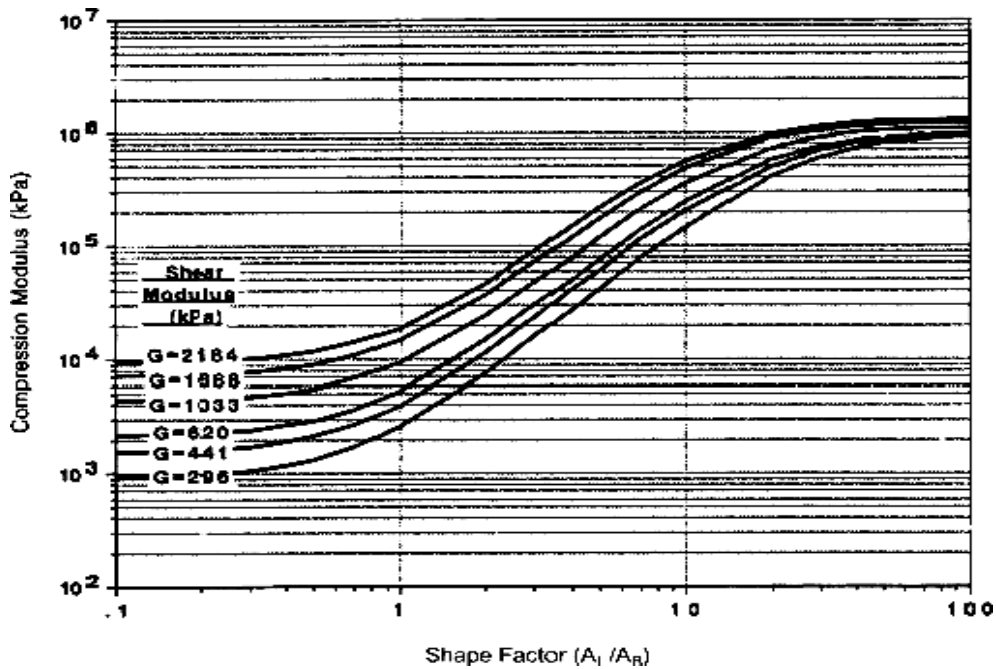


Fig. (5) Compression modulus versus shape factor for various shear modulus [11].

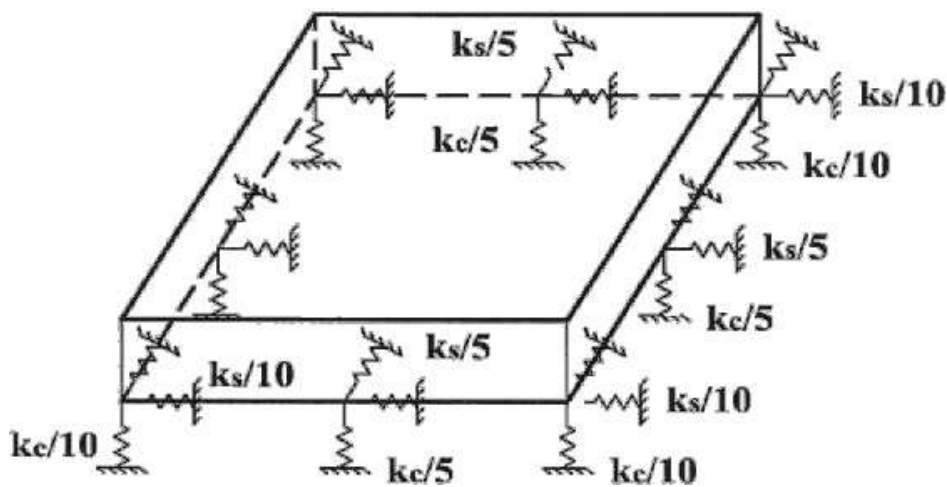


Fig. (6) Representing stiffness of bearing by equivalent springs.

## APPLICATIONS AND DISCUSSIONS

The primary objective of the present investigation is to study the effects of boundary conditions at the supports, and its effects on the behavior of the bridge.

A single span reinforced concrete three-girder bridge has been analyzed by using three types of supports. First one is the simple support represented by a hinge at left ends and roller at the right ends of the girders and in the second case the elastomeric support represented by brick elements, while in the third one simple springs are used to simulate these support.

The bridge chosen for the study has been analyzed under single point load placed at different load positions in addition to the self-weight of the structure.

The predicted response of bridge comprises load-deflection curves, a variation of load distribution factors (LDF) with increasing load, and the reaction components at the different supports.

The bridge has a two-lane with an effective span of 21 m and a total deck width of 8.1 m. The spacing of the three main girders is equal to 2700 mm c/c, and the total depth of these girders (including the deck slab thickness) is equal to 1800 mm.

The two cross beams at the support are assumed to be cast monolithically with the deck slab having for convenience the same depth as that of the main girders. The geometry and details are shown in Fig. (7 a-b).

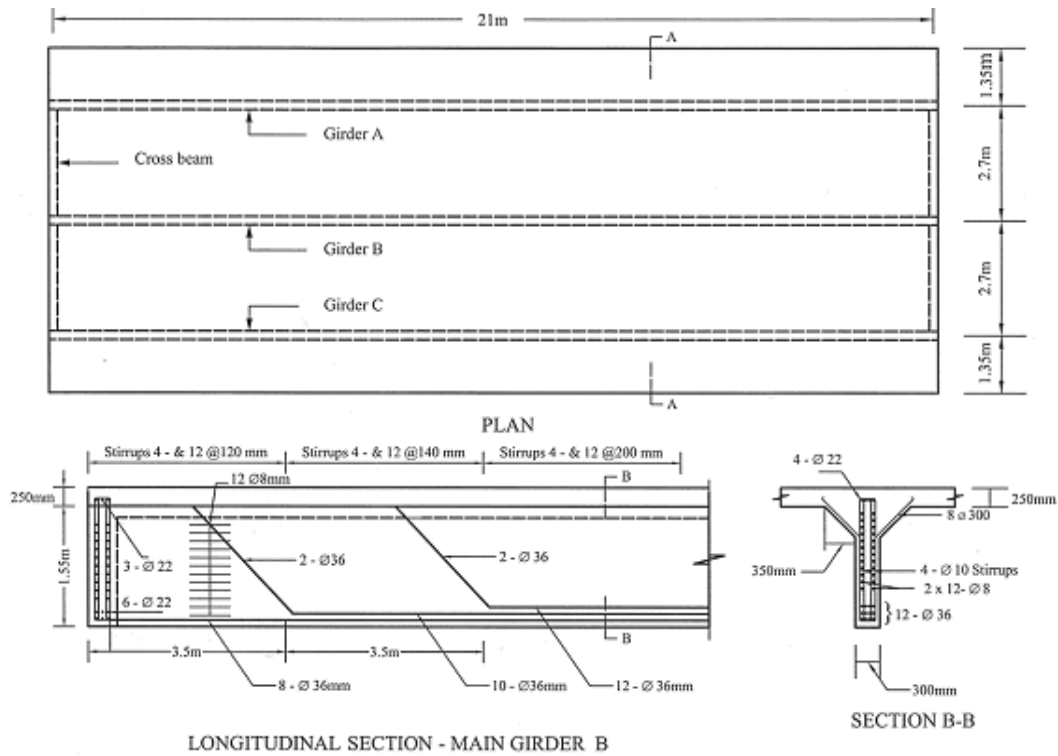
The adopted material properties are summarized in Table (1)

Concrete & Steel						
$E_c$ (MPa)	$f'_c$ (MPa)	$f'_t$ (MPa)	$\nu$	$\epsilon_u$ (MPa)	$E_s$ (MPa)	$f_y$ (MPa)
20700	25	3	0.2	0.0035	196200	415
Elastomeric Bearing						
Rubber			Steel			
$E_o$ (MPa)	$\nu$	$f'_c$ (MPa)	$E_c$ (MPa)	$\nu$	$f_y$ (MPa)	
4.45	0.49	20	200000	0.3	345	

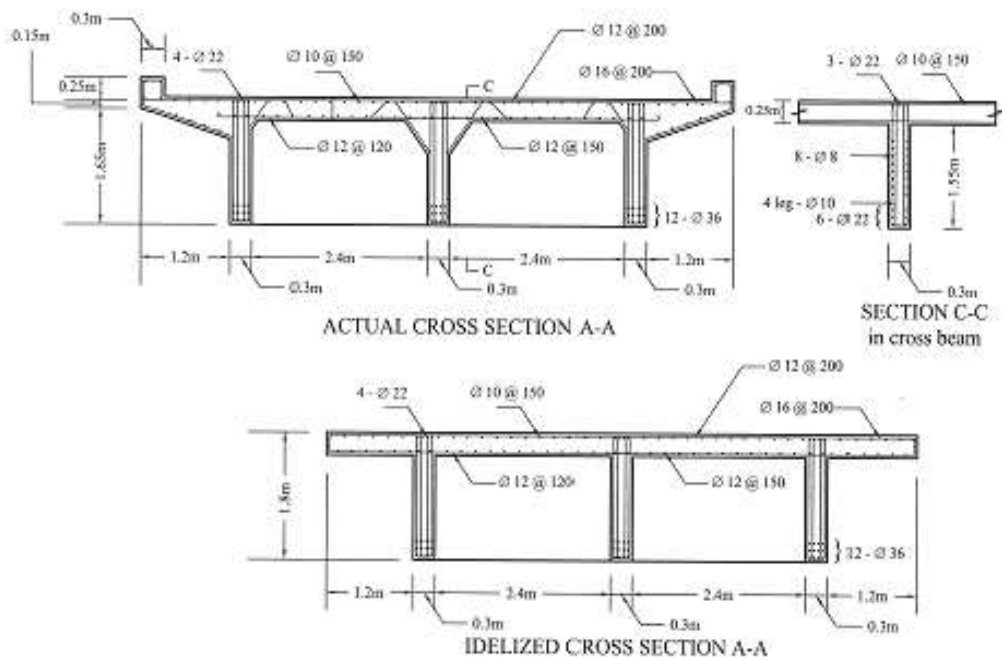
The analysis has been carried out fewer than six different load positions; each load case is assigned a number from L1 to L6 as shown in Fig. (8).

The position of the different sections under study is defined regarding distance X from the roller end of the bridge.

The deck slab has been idealized by 72 brick elements, having nine elements in the transverse direction with widths equal to (1.2, 0.3, 1.2, 1.2, 0.3, 1.2, 1.2, 0.3, 1.2) m.



(a) Plan and a Longitudinal section of the main girder



(b) Actual and idealized cross-section of Bridge

Fig. (7) Detail of the analyzed Bridge (a) and (b)

And 8 elements along the span with lengths equal to (0.3, 3.2, 3.5, 3.5, 3.5, 3.5, 3.2, 0.3) m.

Each longitudinal girder is represented by eight elements along the span, using single element across the depth, while the cross beams have been described by two elements each having 1.2 m length.

This type of bridge is a three-dimensional structure in nature, and different boundary conditions at the end support may significantly affect its behavior [3]. Thus the whole structure has been taken into consideration in the analysis even under symmetrical loading when simple supports (hinge at one end and roller at the other end) are used. When using elastomeric support or springs support, also the whole structure has been analyzed, in spite of the symmetry of boundary conditions at these supports, and that is to compare their response with a simple support bridge.

### Elastic Analysis

For each load case, an elastic analysis is carried out for the bridge under a point load of 1000 KN. From this analysis, the reaction components have been determined, and these are later compared with the same using the nonlinear analysis.

### Nonlinear Analysis

For the six load cases, a nonlinear analysis is carried out for the bridge.

The structure is first subjected to its self-weight which is applied in a single load step, followed by the point load which is implemented in several stages varies between (18 - 23) increments up to failure.

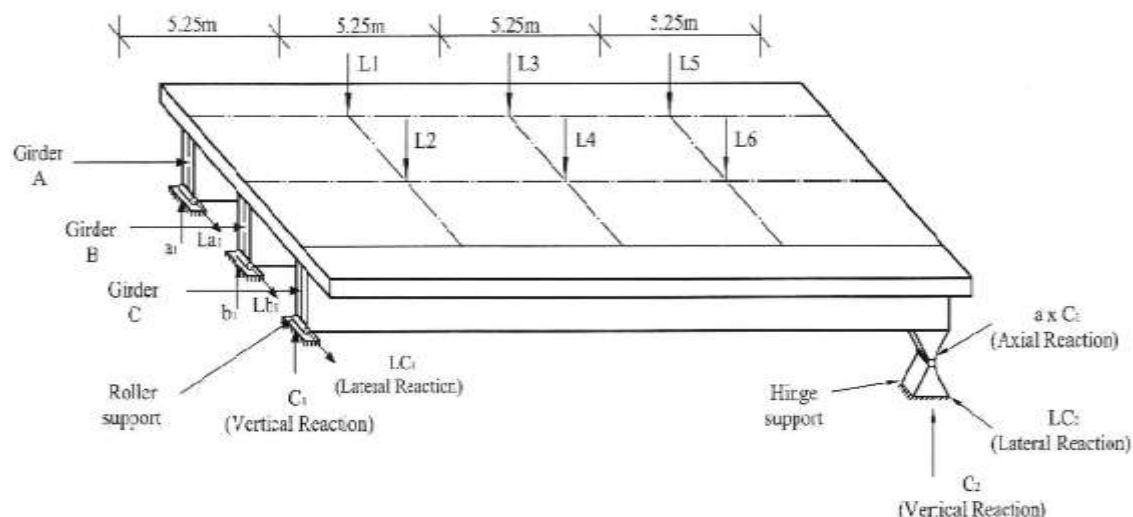


**Fig. (8) Positions of single point live load for six different load cases, L1 to L6.**

### Load Deflection Curves

The predicted load-deflection curves at the point load position, for the analyzed bridges, are shown in Figs. (9a-f).

These figures show the comparison of load-deflection curves for the Bridge with three types

of supports, simple support, elastomeric support and springs support.

It is seen that the deflection at the load position in all load cases for bridges having elastomeric support and springs support is almost identical and it is more flexible compared to the deflection for bridge having simple support, particularly at an eccentric load case (L1, L3, L5).

Due to the symmetry of boundary conditions at both elastomeric and springs support, it is seen that the deflection for a similarly placed loads L1, L5 and L2, L6 are identical as shown in Figs. (9 a,e) And (9 b,f) respectively, while using simple support, there is a quite a significant variation in the deflection for those similarly placed loads (L1 and L5). This may be attributed to the different boundary conditions at the two ends of the bridge, and the axial restraint of the hinge support which causes thereby a reduction in deflections and higher load carrying capacity when the load is close to the hinge support, as shown in Figs. (9 a,e and b,f).

### Variation of LDF with Increasing Loads

The theoretically predicted load distribution factors (LDF) amongst the essential girders at different load stages at selected critical sections are presented in Figs. (10 a - f) for different types of supports under different load cases.

The bending moment in the main girders has been computed by integrating the stress-resultants in concrete as well as in the secondary and main steel. These moments are found first for the dead load, which is the first load step, and under subsequent live load steps. At any particular section, the bending moment due to L.L. alone is determined by subtracting the dead load moment from the corresponding total moment. The LDF at any section of a girder  $i$  is then determined as:

The ratio of live load L.L. moment in girder  $i$  to the average L.L. moment in each girder at that section, this can be expressed as:

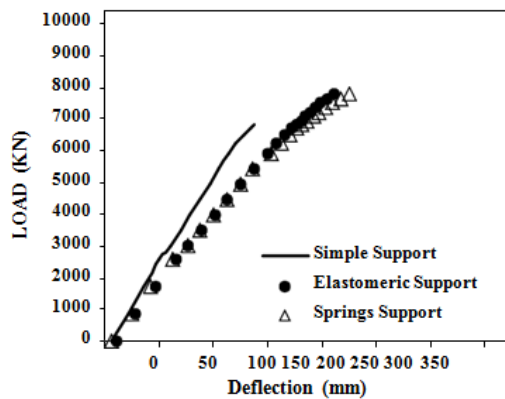
$$LDF \text{ in Girder } i = \frac{L.L \text{ moment in girder } i}{(Total \ L.L \ \text{moment at the section}/n)}$$

Where:

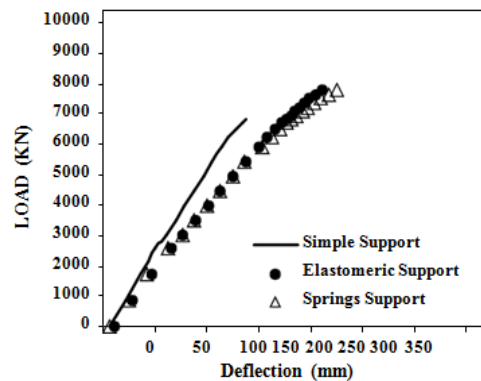
- $n$  is equal to the total number of girders.

The variation of LDF under load cases (L1, L2), (L3, L4) and (L5, L6) are given at sections at distances 7m, 10.5m, and 14m respectively from the roller supports. These sections have been chosen at the Gauss point locations, which are as close as possible to the section where point load is applied.

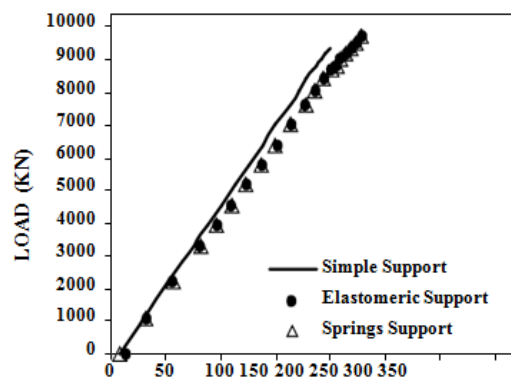
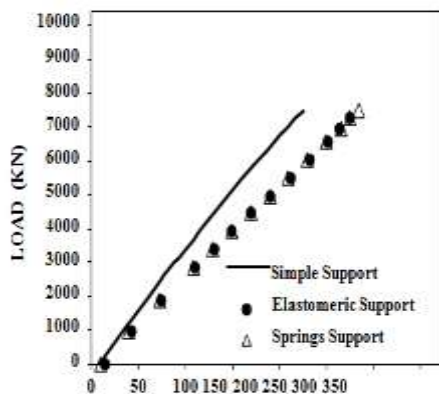
The response of the bridge under different loads is discussed below:



(a) Load case L1



(b) Load case L2



**Load case L1:** The variation of the LDF values in the main girders at section 7m for bridge supported on a simple bearing and bridge supported on the elastomeric bearing is shown in Fig. (10a). It is important to understand that, while using simple support, the L.L. carried by the farthest unloaded girder C is considered to be negligible. The major part of the L.L. (about 66%) is carried by the loaded girder A. The difference in the LDF of girders A and B is also quite significant through all stages of loading. Although this difference gets slightly reduced at a load of 3026 KN at which yielding of the main steel at this section started.

In a series of numerous experiments, similar response for the bridge with elastomeric bearing were successfully predicted except at the elastic stages, where the difference in the LDF values for girders A&B are less in the elastic stages compared with that of a simple support bridge.

**Load case L2:** The variation of the LDF values at the 7m section in the main girders for different types of bearings are shown in Fig. (10b). It is seen that these values in the main girders for both simple and elastomeric support are nearly identical at different stages of loading. It is also clear that the LDF values for the loaded girder B increase up to a load of 3916 KN, at which yielding of the main steel of girder B is started. This causes a redistribution of the load to the outer girder A&C, and the load is almost equally distributed amongst the main girders at this section, this remains true up to failure load.

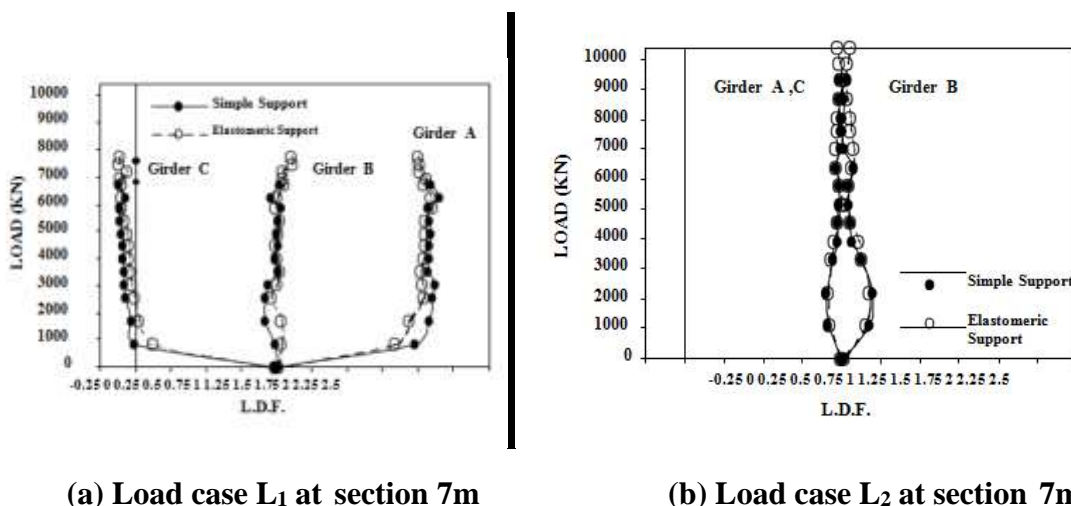
**Load case L3:** In this case the load placed on outer girder A at mid-span.

The load distribution amongst the main girders may see to be very poor right from early stages of loading up to ultimate load for a simply supported bridge as shown in Fig. (10 c). While using elastomeric support, the difference of LDF values in the main girders reduces at elastic stages. Also the same can be noticed near ultimate load stages, and that is due to the redistribution of the load amongst the main girders.

**Load case L4:** Fig. (10 d) Shows that the response of bridge for the two types of bearings is almost identical up to near ultimate load. The LDF values of loaded girder are reduced at a load of 3916 KN when the main steel at this section start is yielding.

It can be seen that near ultimate load stages, the difference in the LDF values for the main girders, when using elastomeric support got reduced due to the redistribution of load to the outer girders A, C at these stages of loading.

**Load case L5:** In this case, as shown in Fig.(10 e), the values of LDF in the main girders of bridge supported on elastomeric bearings are almost same as that under similarly placed load with respect to the mid-span (L1), and that is due to the symmetry of boundary conditions at these supports. While using simple supports (roller & hinge), the difference in the LDF values from load case (L1) is quite significant. The difference in the LDF of girders A and B is also quite significant through all stages of loading.



This may be attributed to the eccentric axial force (axial reaction) at the hinge support which increases when the load moves toward the hinge support. This causes a higher load carrying capacity for loaded girder A of the bridge compared with the symmetrically placed load case (L1). Therefore, in this case, the load carried by the other girders (B & C) is less than that for symmetrically placed load case (L1) for the same bridge.

**Load case L6:** Figure (10 f) gives a clear presentation that variation of LDF values in the main girders for bridge supported on elastomeric bearings are the similar to that under equivalent placed load (L2), this is also due to the symmetry of boundary conditions at both ends of the girders.

Using simple support, the loaded girder B continue to carry large percent of the load up to failure, although the main steel at this section starts yielding at load 3916 KN. The large share of a load of this girder is due to the axial restraint at hinge support near this loaded part as pointed out previously.

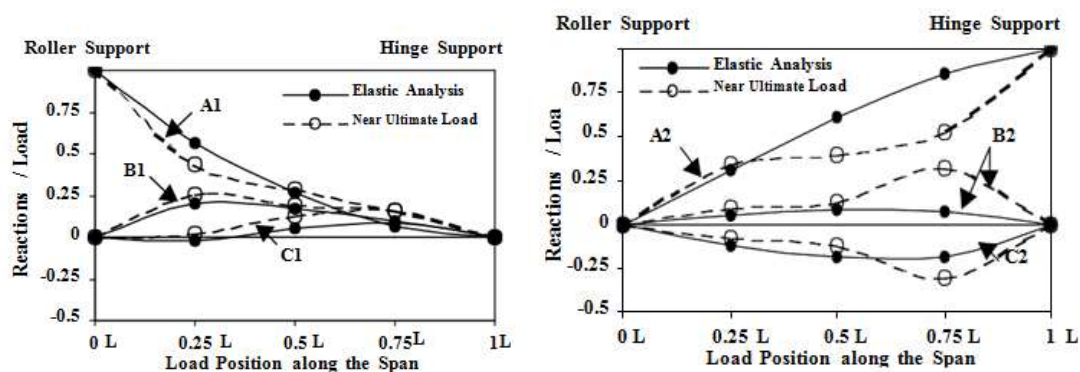
## Vertical Reactions

In this study, the support reactions at the roller and the hinge support of the main girders and reactions for the elastomeric bearings symmetric at both ends of the girder are also predicted at different stages of loading.

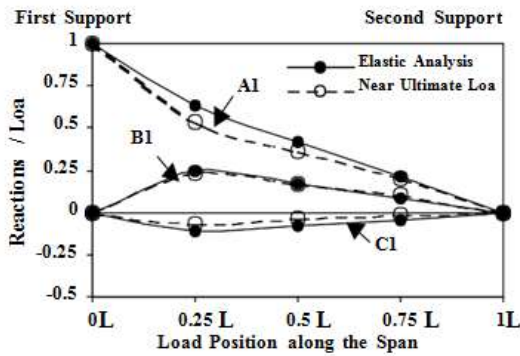
The theoretically obtained vertical reactions are termed as A1, B1, and C1 at the roller support or first elastomeric support, and as A2, B2 and C2 at the hinge support or second elastomeric support, where characters A, B, and C refer to the girders A, B, and C respectively.

These reactions, expressed regarding the applied external load at the elastic and near ultimate load stages, are shown in Figs. (11 - 12). The distribution of the reactions for the load moving along girder A are shown in Figs. (11 a-b) for a simple supports and Figs. (11 c-d) For an elastomeric supports. It can easily be observed that the reaction components under the three girders at the roller end differ only marginally in the elastic stage from that near failure stage. The reactions A1, B1 at the roller supports becomes almost equal in the post-cracking stages when the load passes quarter the span. This is due to the load distribution from the loaded girder A to the adjacent girder B as shown in Fig. (11 a). But reaction components A2, B2 and C2 at the hinge support are significantly differed near failure from that in the elastic stage values as shown in Fig. (11 b) Particularly when the load is at position 0.75L. It is interesting to note that reaction under girder C is negative at the hinge end only when the load moves on the outer girder A. Figs. (11 c-d) Show the symmetry in the reactions under the three girders for both ends of the elastomeric supports, and this is due to the symmetry of the boundary condition at these ends. From these figures, it is seen that the reactions at the first and second elastomeric support differ slightly from the elastic stage to that near failure stage.

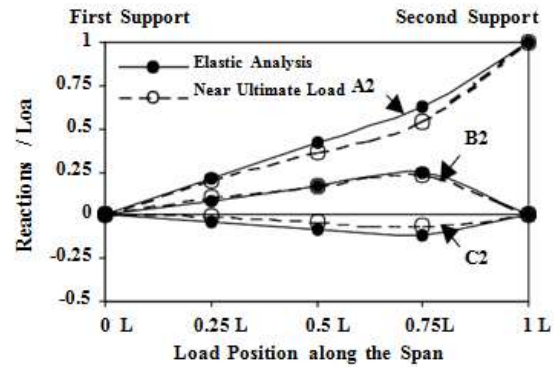
The numerically predicted vertical reaction when the load moves on the central girder B is shown in Figs. (12 a-b) for the roller and the hinge support respectively, and Figs. (12 c-d) For both first and second elastomeric support which are symmetric at the ends. The roller reactions in the elastic stage and near failure are closely similar under all the girders conditions, whereas the vertical reaction at the hinge end under the loaded girder B in the post-cracking stages is less than that in the elastic stages, when the load at position 0.75L in particular, and this due to the load distribution from the loaded girder B to the outer girders A,C at the same section due to the reduction in its stiffness. The reactions at the first and the second elastomeric support are closely similar under all the girders conditions in the elastic stages and near failure as presented in Figs. (12c-d).



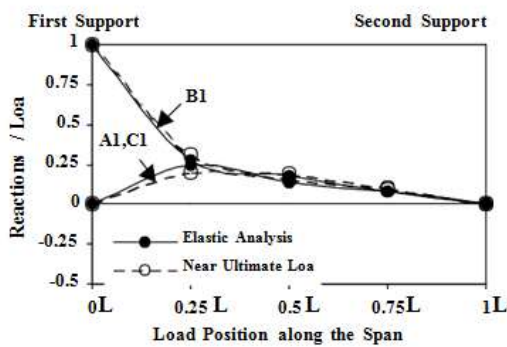
(a) Roller support



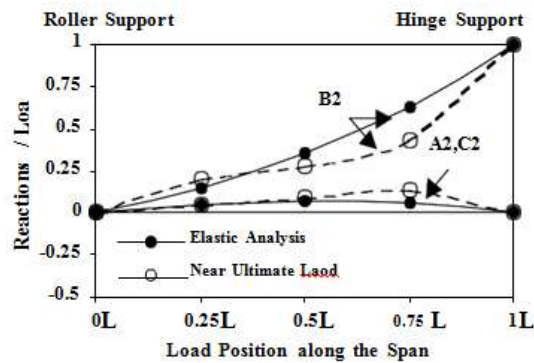
(b) Hinge support



(c) First elastomeric support



(d) Second elastomeric support



(a) Roller support

(b) Hinge support

## CONCLUSIONS

The method presented in this paper is capable of idealizing the T-beam Bridge close to its actual physical structural properties. Based on the analytical results and critical discussion of the results the followings can be concluded:

- 1) The load-deflection curves for bridge supported on elastomeric supports and springs support are almost identical and show more flexibility compared to the load-deflection curves for bridge supported on a simple supports especially at an eccentric load case (L1, L3, L5).
- 2) The different boundary conditions at the ends of the simply supported bridge cause the unsymmetrical behavior of bridge under symmetrically placed loads. This is due to the axial restraining at the hinge support which causes a reduction in the deflection and increasing ultimate load capacity when the load is in the vicinity of the hinge supports.
- 3) For the cases when the load approaching the hinge support, the distribution of the load amongst the main girders at the loader section, using elastomeric support, is better than that of the classical hinge- roller support.

**Notations**

<b><math>A</math></b>	<b>Loaded area</b>
<b><math>[B]</math></b>	<b>Strain-displacement matrix</b>
<b><math>[D]</math></b>	<b>Elasticity constitutive matrix of concrete</b>
<b><math>[D_s]</math></b>	<b>Elastic or elastic-plastic material matrix of the smeared steel layer</b>
<b><math>d_c</math></b>	<b>Compression displacement</b>
<b><math>d_s</math></b>	<b>Shear displacement</b>
<b><math>E_c</math></b>	<b>Initial modulus of elasticity of concrete</b>
<b><math>E_s</math></b>	<b>Initial modulus of elasticity of steel</b>
<b><math>E_o</math></b>	<b>Young's Modulus of rubber</b>
<b><math>F_c</math></b>	<b>Applied force in the compression direction</b>
<b><math>F_s</math></b>	<b>Applied force in the shear direction</b>
<b><math>f'_t</math></b>	<b>The uniaxial tensile strength of concrete</b>
<b><math>f'_c</math></b>	<b>The uniaxial compressive strength of concrete</b>
<b><math>F_y</math></b>	<b>The yield strength of steel</b>
<b><math>G</math></b>	<b>The shear modulus of the rubber</b>
<b><math>[J]</math></b>	<b>Jacobian matrix</b>
<b><math>[K_T]</math></b>	<b>Global tangent stiffness matrix</b>
<b><math>[K_c]</math></b>	<b>Concrete stiffness matrix</b>
<b><math>[K_s]</math></b>	<b>Steel stiffness matrix</b>

**REFERENCES**

- [1] Bakht, B. and Jaeger, L. G., "Bearing Restraint In Slab-on-Girder Bridges," Journal of Struct. Engng. Vol. 114, No. 12, Des 1988.
- [2] Kassim, M., Tarhini and Gerald, Frederic R., "Load Distribution on Highway Bridges Using ICES-STRUDL Finite Element Analysis," Computers and Struct. Vol. 32, No. 6, 1989, PP. 1419-1428.
- [3] Mahmood, M. N., "Investigation of Post-Cracking Behaviour of Reinforced Concrete Girder Bridge," Ph. D. Thesis, University of Roorkee, India, 1994, 247, PPs.
- [4] Kwasniewski, L., "Sensitivity Analysis for Slab-on-Girder Bridges," 8th ASCE Special Conference on Probabilistic Mechanics and Structural. Reliability PM 2000-319.
- [5] Embabi, M. S., and Cope, R. J., "An Equivalent Elasto-Plastic Constitutive Model for Biaxially Loaded Concrete," Proceeding of International Conference on Computer Aided Analysis and Design of Concrete Structures, Pineridge Press Limited, Swansea, 1984, PP. 275- 288.
- [6] Cervera, M. and Hinton, E., "Nonlinear Analysis of Reinforced Concrete Plate and Shell Structures" Using 20-Noded Isoparametric Brick Elements", International Journal of Computers and Structures, Vol. 25, No. 6, 1987, PP. 845-869.
- [7] Owen, D. R. J., and Hinton, E., "Finite Element in Plasticity: Theory and Practice," Pineridge Press Limited, Swansea, U.K., 1980.
- [8] Vector, D. T., "Essentials of Bridge Engineering," Fourth Edition, Oxford and IBH Publishing Co. Pvt. Ltd. 1991.
- [9] Lakes, R. S., "Design Considerations for Negative Poisson's ratio Materials" ASME Journal of Mechanical Design, 115, 1993, PP. 696-700.
- [10] Lindley, P. B., "Engineering Design With Rubber," MRPRA, Table 3, P. 8, 1978.
- [11] Gent, A. N., "Engineering with Rubber: How to Design Rubber Components," 2nd

edition, CH. 8, Jun. 2001, PP. 224-232.

- [12] Zienkiewics, O. C., "The Finite Element Method," McGraw-Hill, Third Edition, London, 1977.
- [13] Jallo, E.K., "Effect of Types of Bearing on the Load Distribution Among Girders of the Bridge," MSc. Thesis, 2004
- [14] Irons, B. M., "Quadrature Rules for Brick-Based Finite Elements," Investigational Journal for Numerical Methods in Engineering, Vol. 3, 1971, PP.293.